

# Characterization of Oil Palm Shell Activated Carbon and ZSM-5 Supported Cobalt Catalysts

Izirwan I.<sup>1,2\*</sup>, Mohd A.<sup>1</sup> and Saidina Amin N.A.<sup>1</sup>

1. Chemical Reaction Engineering Group (CREG), Energy Research Alliance, Faculty of Chemical Engineering, Universiti Teknologi Malaysia, 81310 Johor Bahru, Johor, MALAYSIA.

2. Faculty of Chemical Engineering and Natural Resources, Universiti Malaysia Pahang, Lebuhraya Tun Razak, 26300 Gambang, Kuantan, Pahang, MALAYSIA.

\*izirwan@ump.edu.my

## Abstract

*In this paper we are reporting the preparation and characterization of supported cobalt catalysts using a wetness impregnation method. Different cobalt catalysts loading of 0 and 10 wt% were prepared by dissolving cobalt nitrate hexahydrate in distilled water and dried in an oven at 100 °C overnight. Two selected supports of oil palm shell (OPS) activated carbon and ZSM-5 zeolite were employed and compared. Catalysts characterizations of both supports were performed by thermogravimetric analysis (TGA), X-ray diffraction (XRD) analysis and scanning electron microscope analysis (SEM). Using Scherrer equation, the cobalt metallic size was calculated. OPS activated carbon supports were further analyzed for CHNOS elemental analysis. Both supports of OPS activated carbon and ZSM-5 zeolite exhibited the successful loading of cobalt catalysts and have potential to be utilized in catalytic reactions.*

**Keywords:** Activated carbon, cobalt catalyst, oil palm shell, zeolite, ZSM-5.

## Introduction

Cobalt based catalysts are widely employed for catalytic reactions<sup>1-2</sup> due to their high activity<sup>3-5</sup>, less side reactions such as low water-gas shift activity<sup>6</sup> and high selectivity of desired products<sup>7-11</sup>. Other available metal catalysts especially the transition metals such as Ru, Pd, Pt are superior in their reaction performances but because of expensive in price hinder their utilization in the large scale for industrial production. Cobalt catalysts are comparatively cheaper and reasonable in price<sup>12</sup> than the transition metals with good reaction performances.

In order to improve the catalyst activity and selectivity, the cobalt precursor is dispersed onto the surface of the porous supports to enhance the catalytic surface area for the successive reactions. Various methods of catalysts loading such as ultrasound impregnation<sup>13</sup>, incipient wetness co-impregnation<sup>14</sup> are employed for loading the catalysts onto the supports. The porous supports such as ZSM-5 zeolite, activated carbon, alumina, titania, bentonite, and silicon carbide<sup>15</sup> are selected for the augmentations of the catalysts surface area, pore diameter, pore volume and metal-support interaction that have a great effect on the size, dispersion and catalytic performance of cobalt catalysts.

The objective of this study is to prepare and characterize the cobalt catalysts based on the different supports of ZSM-5 zeolite and OPS activated carbon with various loadings of cobalt catalysts.

## Material and Methods

**Chemicals:** Zeolite and activated carbon were used as supports for catalysts. Zeolite ammonium ZSM-5 powder was purchased from Zeolysts International. Activated carbon of Oil Palm Shell (OPS) was supplied by Multi Filter Sdn Bhd. The precursor of cobalt catalysts was cobalt (II) nitrate hexahydrate,  $\text{Co}(\text{NO}_3)_2 \cdot 6\text{H}_2\text{O}$  from Friendemann Schmidt.

**Catalysis Synthesis:** The oil palm shell (OPS) activated carbon was rinsed with distilled water to remove impurities and dried in an oven at 110 °C overnight. The cobalt precursor was added onto the supports of

OPS activated carbon by wetness impregnation method after dissolving in distilled water. The mixtures were stirred on a magnetic stirrer plate overnight. Then, the sample was dried in the oven at 110 °C for 3 days. As for support of ZSM-5, this zeolite was utilized without further treatment and using the aforementioned method of catalysts loading. Only ZSM-5 zeolite supported cobalt catalysts were calcined at 550 °C for 5 h at a heating rate of 10 °C/min in a furnace. Both supported cobalt catalysts were prepared at different cobalt loadings of 0 and 10 wt% and denoted as AC(0), AC(10), ZSM-5(0) and ZSM-5(10) respectively.

**Elemental Analysis:** The elemental analysis of activated carbon was performed by CHNOS Elemental Analyzer Vario MACRO Cube using an oil method.

**Thermalgravimetric Analysis (TGA):** Perkin Elmer TGA7 and Perkin Elmer Thermal Analysis Controller TAC7/DX were used for the thermalgravimetric analysis (TGA). The equipment conditions were set at temperature 29-950 °C, heating rate 10 °C/min and nitrogen flowrate 20 ml/min.

**X-Ray Diffraction (XRD):** X-Ray Diffraction (XRD) analysis was conducted by using a benchtop X-Ray Diffractometer Rigaku Miniflex II with  $\text{Cu}_{K\alpha}$  radiation ( $\lambda_a = 0.1541$  nm), step size 0.02 and scan speed 0.3 s/step. The X-ray tube was operated at 10 kV and at 50pA.

**Scanning Electron Microscopy (SEM):** The surface morphology of the catalysts was observed with a Scanning Electron Microscope (SEM, Zeiss EV050). The images were captured in SEM mode at 5,000 times magnification.

## Results and Discussion

The elemental contents of Oil Palm Shell (OPS) activated carbon were analyzed and the obtained data were shown in table 1. The major elemental content was carbon (C) with the highest percentage of 81.06 wt%. However, the oxygen (O) was calculated at 15.88 wt% by the difference of overall contents. There was a minimal sulfur found at 0.16 wt%

Figure 1 displays the TGA/DTG of OPS activated carbon and activated carbon supported catalyst under  $\text{N}_2$  atmosphere. Generally, a weight loss below 100 °C as exhibited in figure 1 (a) is considered due to the evaporation of the absorbed water in the sample. The activated carbon sample is stable below 650 °C. However, approximately 5% weight loss can be detected when the activated carbon supported cobalt catalyst is heated at 650-700 °C. This is maybe due to the loss of the carbon by oxidation reaction.

Figure 2 shows the TGA/DTG of ZSM-5 zeolite and ZSM-5 zeolite supported catalyst under  $\text{N}_2$  atmosphere. Both curves exhibit a weight loss below 100 °C due to the release of the absorbed water in the samples. The ZSM-5 zeolite sample is thermally unstable with the weight loss of 10 wt% after 650 °C. On the contrary, the ZSM-5 zeolite supported cobalt catalyst sample shows greater stability than the former sample.

Figure 3 presents the XRD patterns of the ZSM-5 zeolite with and without loading of cobalt catalysts. The major magnitude of the peak was observed at 23 degree ( $2\theta$ ) with the intensity of 1800 cps. After the impregnation of cobalt catalysts, the magnitudes of ZSM-5 zeolite peaks were reduced to almost half, indicating that the cobalt catalysts have been successfully coated onto the surface of ZSM-5 zeolite. In addition, the spinel phase of cobalt oxide ( $\text{Co}_3\text{O}_4$ ) was observed at  $2\theta$  of 30.2, 37.0, 45.2, 58.3 and 65.4. The crystallite diameters of cobalt particles were calculated using Scherrer equation taken from the most intense cobalt oxide,  $\text{Co}_3\text{O}_4$  peak at  $2\theta$  of 37.0 as shown below:

$$d = 0.89\lambda/B \cos \theta \times 180/\pi \quad (1)$$

Where d is the mean cobalt crystallite diameter,  $\lambda$  is the X-ray wave length (1.541 Å), and B is the full

(2)

width half maximum (FWHM) of the  $\text{Co}_3\text{O}_4$  diffraction peak. The mean crystallite diameter of the cobalt catalyst was calculated by using (1) and the crystallite diameter was about 0.34 nm.

Figure 4 displays the XRD patterns of the OPS activated carbon with the loading 0 and 10 wt% cobalt catalysts. The major magnitude of the broadening peak was observed at 23 degree ( $2\theta$ ) with the intensity of 650 cps. This magnitude of the broadening peak was reduced to 200 cps, suggesting that the impregnation of cobalt catalysts have been successfully coated onto the surface of OPS activated carbon. However, the spinel phase of cobalt oxide was not obvious due to the broadening of the XRD peaks. Therefore, calculating the size of the cobalt catalyst crystallites using the most intense peak of cobalt oxide may not be accurate for the OPS activated carbon.

The SEM images of OPS activated carbon with and without the addition of cobalt catalysts were presented in Figure 5. As shown in Figure 5 (a), the pores are obviously discovered on the surface of OPS activated carbon in different sizes. After the impregnation with the cobalt catalysts, the pores of OPS activated carbon were completely covered with cobalt particles as shown in Figure 5 (b). Furthermore, the cobalt particles of the catalysts were found to be partly agglomerated on the surface and showed non-uniform distributions.

Figure 6 exhibits the SEM images of ZSM-5 zeolite for 0 and 10 wt% cobalt catalyst loadings. The dense surface morphology was caused by the aggregation of zeolite particles. The existence of cobalt catalyst particles was hardly differentiated but the aforementioned decrease in intensity of XRD peaks suggesting the impregnation of cobalt catalysts.

## Conclusion

Further characterizations of the catalysts are required for the full understandings of the physical and chemical properties of the catalysts. The catalyst supports of OPS activated carbon and ZSM-5 demonstrated the successful loading of cobalt catalysts. In the extensions of this work, both supports of OPS activated carbon and ZSM-5 will be utilized in the catalytic reactions of Fischer-Tropsch synthesis or carbon dioxide reforming of methane.

## Acknowledgement

The authors are grateful to Zainab Salleh from the Faculty of Chemical Engineering, Universiti Teknologi Malaysia for conducting catalyst analyses. This work was supported by Research Energy Alliance of Universiti Teknologi Malaysia under Grant GUP05J02. One of the authors is gratefully acknowledged to the Malaysia Ministry of Higher Education for the scholarship during his study period.

## References

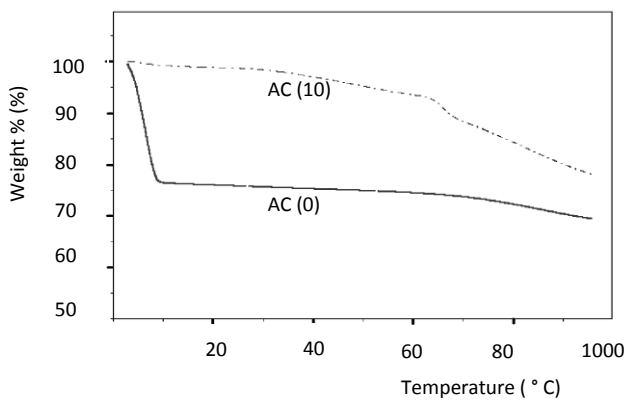
1. Tao C., Li J., Zhang Y. and Liew K.Y., Effect of isomorphic substitution of zirconium on mesoporous silica as support for cobalt Fischer-Tropsch synthesis catalysts. *J. Mol. Catal. A: Chem.* **331**(1-2): p. 50-57 (2010)
2. Knochen J., Güttel R., Knobloch C. and Turek T., Fischer-Tropsch synthesis in milli-structured fixed-bed reactors: Experimental study and scale-up considerations. *Chem. Eng. Process: Process.* **49**(9): p. 958-964 (2010)
3. Tan K.F., Chang J., Borgna A. and Saeys M., Effect of boron promotion on the stability of cobalt Fischer-Tropsch catalysts. *J. Catal.* **280**(1): p. 50-59 (2011)
4. Karimi A., Pour A.N., Torabi F., Hatami B., Tavasoli A., Alaei M.R., and Irani M., Fischer-Tropsch synthesis over ruthenium-promoted  $\text{Co}/\text{Al}_2\text{O}_3$  catalyst with different reduction procedures. *J. Nat. Gas Chem.* **19**(5): p. 503-508 (2010)

5. de la Osa A.R., De Lucas A., Díaz-Maroto J., Romero A., Valverde J.L., and Sánchez P., FTS fuels production over different Co/SiC catalysts. *Catal. Today*. **187**(1): p. 173-182 (2012)
6. Tehrani S., Irani M., Tavasoli A., Mortazavi Y., Khodadadi A.A., and Pour A.N., Studies on accelerated deactivation of ruthenium-promoted alumina-supported alkalized cobalt Fischer-Tropsch synthesis catalyst. *J. Nat. Gas Chem.* **20**(1): p. 65-71 (2011)
7. Bao A., Li J. and Zhang Y., Effect of barium on reducibility and activity for cobalt-based Fischer-Tropsch synthesis catalysts. *J. Nat. Gas Chem.* **19**(6): p. 622-627 (2010)
8. Zakeri M., Samimi A., Khorram M., Atashi H. and Mirzaei A., Effect of forming on selectivity and attrition of co-precipitated Co-Mn Fischer-Tropsch catalysts. *Powder Technol.* **200**(3): p. 164-170 (2010)
9. Khobragade M., Majhi S. and Pant K.K., Effect of K and CeO<sub>2</sub> promoters on the activity of Co/SiO<sub>2</sub> catalyst for liquid fuel production from syngas. *Appl. Energy*. **94**(0): p. 385-394 (2012)
10. Jiao G., Ding Y., Zhu H., Li X., Li J., Lin R., Dong W., Gong L., Pei Y., and Lu Y., Effect of La<sub>2</sub>O<sub>3</sub> doping on syntheses of C1-C18 mixed linear  $\alpha$ -alcohols from syngas over the Co/AC catalysts. *Appl. Catal., A: Gen.* **364**(1-2): p. 137-142 (2009)
11. Cai Z., Li J., Liew K. and Hu J., Effect of La<sub>2</sub>O<sub>3</sub>-dopping on the Al<sub>2</sub>O<sub>3</sub> supported cobalt catalyst for Fischer-Tropsch synthesis. *J. Mol. Catal. A: Chem.* **330**(1-2): p. 10-17 (2010)
12. Lögberg S., Lualdi M., Järås S., Walmsley J.C., Blekkan E.A., Rytter E., and Holmen A., On the selectivity of cobalt-based Fischer-Tropsch catalysts: Evidence for a common precursor for methane and long-chain hydrocarbons. *J. Catal.* **274**(1): p. 84-98 (2010)
13. Zhou X., Chen Q., Tao Y. and Weng H., Influence of Ultrasound Impregnation on the Performance of Co/Zr/SiO<sub>2</sub> catalyst during Fischer-Tropsch Synthesis. *Chinese J. Catal.* **32**(6-8): p. 1156-1165 (2011)
14. Enger B.C., Fossan Å.-L., Borg Ø., Rytter E. and Holmen A., Modified alumina as catalyst support for cobalt in the Fischer-Tropsch synthesis. *J. Catal.* **284**(1): p. 9-22 (2011)
15. de la Osa A.R., De Lucas A., Romero A., Valverde J.L. and Sánchez P., Influence of the catalytic support on the industrial Fischer-Tropsch synthetic diesel production. *Catal. Today*. **176**(1): p. 298-302 (2011)
16. Daud W.M.A.W., Ali W.S.W. and Sulaiman M.Z., The effects of carbonization temperature on pore development in palm-shell-based activated carbon. *Carbon*. **38**(14): p. 1925-1932 (2000)

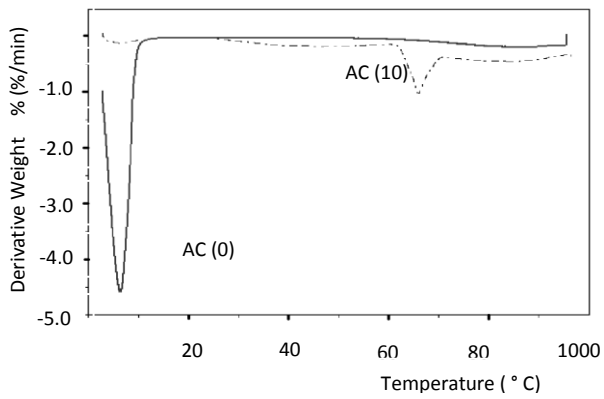
**Table 1**  
**Ultimate analysis of activated carbon**

Elemental Analysis (wt.%)				
C	H	N	S	O
50.10	6.85	1.90	ND* <sup>16</sup>	41.15
81.06	1.78	1.12	0.16	15.88

\*ND, not detectable

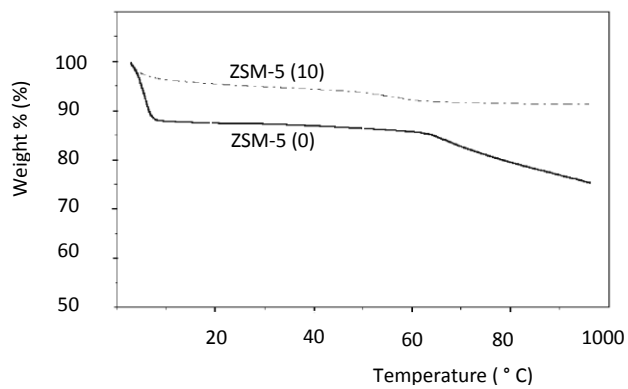


(a)

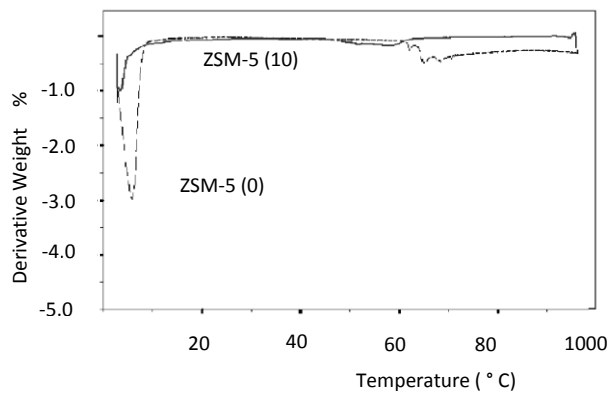


(b)

**Fig.1: TGA/DTG curves of activated carbon: (a) TGA ; (b) DTG.**

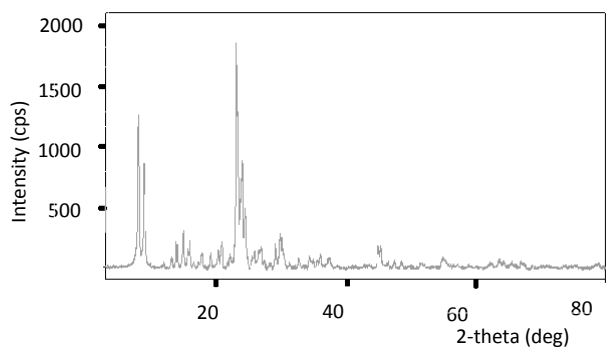


(a)

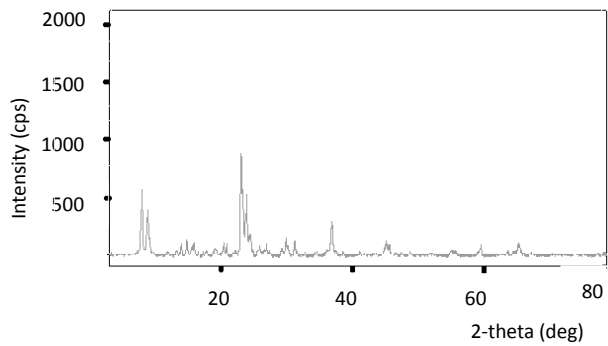


(b)

**Fig. 2: TGA/DTG curves of Zeolite ZSM-5: (a) TGA ; (b) DTG.**



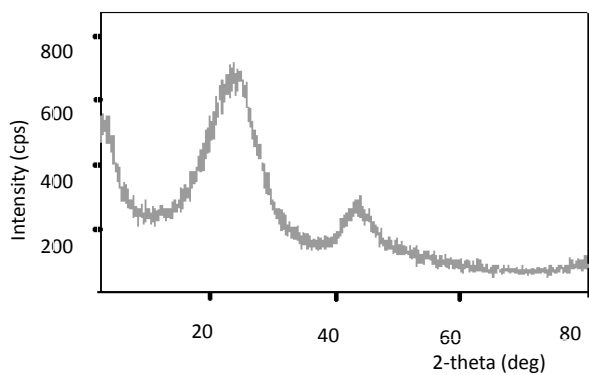
(a)



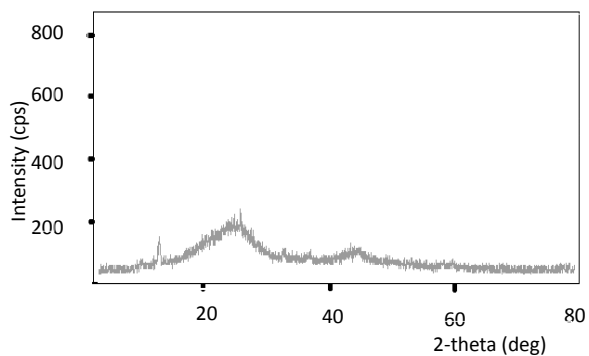
(b)

**Fig. 3: XRD patterns of Zeolite ZSM-5: (a) ZSM-5(0) ; (b) ZSM-5 supported cobalt catalyst, ZSM-5(10).**

(6)

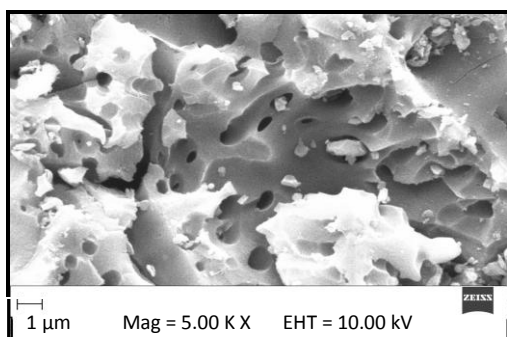


(a)

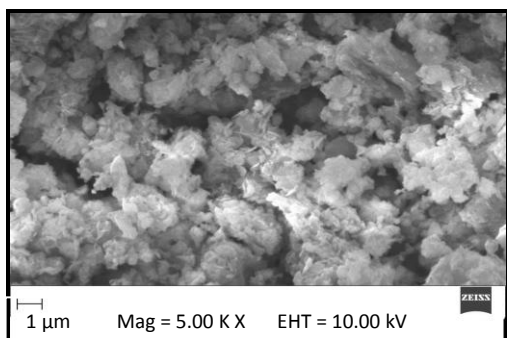


(b)

**Fig. 4: XRD patterns of: (a) activated carbon, AC(0) ; (b) activated carbon supported cobalt catalyst, AC(10).**

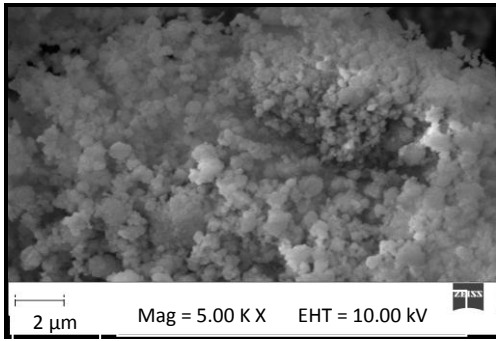


(a)

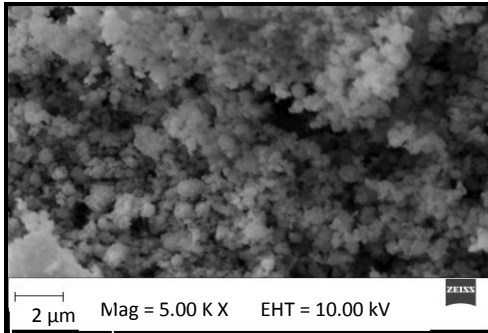


(b)

**Fig. 5: SEM images of activated carbon at 5000x magnification: (a) activated carbon ; (b) activated carbon supported cobalt catalyst.**



(a)



b)

**Fig. 6: SEM images of Zeolite ZSM-5 at 5000x magnification: (a) ZSM-5 ; (b) ZSM-5 supported cobalt catalyst**